Journal of Applied Physics

AIP Publishing

Mechanical and optical response of polymethylpentene under dynamic compression

L. M. Barmore[a)]

Department of Physics and Astronomy, Washington State University, Pullman, Washington 99164, USA and

Institute for Shock Physics, Washington State University, Pullman, Washington 99164, USA

M. D. Knudson[b)]

Institute for Shock Physics, Washington State University, Pullman, Washington 99164, USA

(Dated: 16 October 2019)

Polymethylpentene, commonly referred to by its trade name TPX (Mitsui Chemicals, Inc.), is a thermoplastic polymer that has the potential to be a useful window material for dynamic compression experiments. For such experiments, an optically transparent or low x-ray absorptive window is often used to maintain stress within the sample during compression. TPX can be used as a low-impedance optical and x-ray window due to its good transmittance in most parts of the electromagnetic spectrum, very low density (0.83 g/cm^3), and low x-ray absorption. In dynamic compression experiments interferometry can be used to determine the particle velocity at the interface between the sample and window. However, velocimetry measures the rate of change of the optical path length, commonly referred to as the apparent particle velocity. An experimentally determined window correction factor is needed to ascertain the actual particle velocity from the measured apparent velocity. Here we present the results of a series of dynamic compression experiments from 1 to 31 GPa designed to characterize the mechanical and optical response of TPX, determine the range of stresses over which TPX is transparent, and determine the window correction factor. The index of refraction was found to be essentially linear in density, resulting in a simple constant correction factor. TPX was found to remain largely transparent over the entire stress range examined.

[a)]Electronic mail: lauren.barmore@wsu.edu

[b)]Present address: Sandia National Laboratories, Albuquerque, NM 87185-1195

I. INTRODUCTION

Polymethylpentene, or poly(4-methyl-1-pentene) (PMP), commonly referred to by its trade name TPX (Mitsui Chemicals, Inc.), is a transparent thermoplastic polymer with chemical formula C_6H_{12} and density of 0.83 g/cm^3. It exhibits approximately 90% transmittance at 532 nm and 1550 nm wavelengths[1,2] and the ambient refractive index, $n_0 = 1.462$, is relatively independent of wavelength in this range.[3] Additionally, it exhibits rather low x-ray absorption. TPX is commercially available, easily machined to any desired size, and not affected by limited contact with solvents such as water, isopropanol, or acetone. These attributes make TPX an excellent candidate for a low-impedance window material in dynamic compression experiments.

For use as an optical or x-ray window, TPX would be affixed to a sample and dynamically compressed. Interferometry can be used to measure the Doppler-shifted light reflected from the interface between the sample and window. Common interferometry techniques used in dynamic compression experiments are VISAR[4] (Velocity Interferometer System for Any Reflector) and PDV[5] (Photon Doppler Velocimetry), which typically use 532 nm and 1550 nm wavelength light, respectively. These measurement techniques provide the rate of change of the optical path length, commonly referred to as the apparent particle velocity. A window correction factor, which is contingent on the dependence of the index of refraction on density, is needed to ascertain the actual particle velocity from the measured apparent velocity. The dependence of refractive index on density in TPX is unknown. Results from dynamic compression experiments can be used to determine the density and refractive index at various stresses.

Past studies[6,7] have focused on the behavior of TPX in the terahertz range at ambient conditions. The optical properties of TPX have not been widely studied in the visible and near infrared regime; in particular it is not known how the refractive index depends on the density. Furthermore, there have been few studies performed to investigate the response of TPX under dynamic compression. Aslam et al.[8] performed multi-shock compression and release experiments on TPX to determine the equation of state, but the Hugoniot response was not examined. Haill et al.[9] modeled the behavior of shocked TPX foam rather than full-density TPX. Earlier experiments,[10] performed in the 1980s, examined the mechanical response of TPX under dynamic compression, but did not investigate the optical response. Density functional theory (DFT) and molecular dynamics simulations of the Hugoniot for TPX were found to be in agreement with these experiments.[11] More recently, Root et al.[12] studied the mechanical response of TPX at very high stresses (100-1000

GPa); in this stress range TPX was found to become reflective so interferometry measurements provide direct determination of the shock velocity. Understanding the optical properties of TPX at lower stresses - where TPX remains optically transparent - will enable its use as a window material, since knowledge of the window correction factor will enable the actual particle velocity to be determined.

Here we present the results from a series of dynamic compression experiments on TPX designed to characterize the mechanical and optical response in the stress range of 1 to 31 GPa. Single-stage and two-stage gas-gun experiments and powder gun experiments were performed with both TPX and copper impactors. Measurement of the shock velocity and apparent particle velocity, along with the inferred particle velocity obtained from impedance matching,[13] enabled determination of the stress, density, and index of refraction. The index of refraction was found to be essentially linear in density, resulting in a simple constant correction factor. TPX was also found to remain largely transparent over the entire stress range examined.

II. EXPERIMENTAL CONFIGURATION

A series of dynamic compression experiments was performed by impacting TPX samples with either TPX or copper impactors using a powder or light gas gun. The lower stress experiments were prepared as symmetric impact experiments, with TPX disks directly impacted onto TPX samples using both a 101.6 mm bore single-stage gas gun and 25.4 mm bore two-stage gas gun. The higher stress experiments used a copper impactor and were performed on a 30.5 mm bore powder gun and the 25.4 mm bore two-stage gas gun. Two different grades of TPX were examined. The first was believed to be RT18 obtained from Adamas Optics. The second was DX845 obtained from Goodfellow. The grades of TPX are manufacturer designations that indicate differences in melt flow rate and suitability for different molding processes. The 1 GPa experiment on the 101.6 mm bore gun was repeated with both grades of TPX to evaluate any differences between the grades. No significant differences were observed. Since DX845 is more commonly used (Root et al.[12] also used DX845), we chose to use that grade in all subsequent experiments.

FIG. 1 Front and side views of the "top hat" configuration of TPX sample. Arrows on the side view show the location of velocimetry probe measurements.

The TPX samples were machined from a stock 25.3 mm diameter rod, lapped and polished until

the surface was optically smooth. Density was computed from the measured mass and volume of the sample and was found to be 0.831 g/cm^3 for grade DX845 with an uncertainty of 0.1%. For all experiments, the sample was prepared in a "top hat" configuration, as shown in Figure 1. A 25.3 mm diameter TPX buffer was backed by an 8 mm diameter TPX window. Both buffer and window were nominally 2.75 mm thick and each had a layer of aluminum, approximately 400 nm thick, vapor deposited on the front surface. The pieces were bonded with a thin layer of EPON 815 epoxy. Bond thicknesses were determined to be on the order of a few microns or less. The ambient material properties, including density and sound speed for each material, are recorded in Table I. The measured thicknesses of the impactor, buffer, and window for each experiment are listed in Table II.

The samples were diagnosed using velocity interferometry, both VISAR (532 nm) and PDV (1550 nm). Four interferometry probes were used, as shown in Fig. 1; these included one combination VISAR/PDV probe in the center to measure the apparent velocity at the interface between the buffer and window, and two PDV probes and one combination VISAR/PDV probe at a 9.5 mm radius to measure the apparent velocity at the impact surface. Ambiguity in the measured fringe shift was mitigated through the use of two different VISAR sensitivities or velocity per fringe (vpf) settings for each experiment. The vpf settings in these experiments ranged from 0.117 to 1.036 km/s/fringe. The three PDV probes at the 9.5 mm radius allowed for determination of the impactor tilt and an estimate for the impact time at the center of the sample through interpolation. Typical values for impactor tilt were approximately 2 mrad, but this varied depending on which launcher was used (ranged from 0.369 to 12.90 mrad).

The impact velocity on the 101.6 mm bore gun was recorded just prior to impact with pins that were electrically shorted upon contact with the projectile as it traveled down the barrel. The 25.4 mm bore two-stage gun and the 30.5 mm bore powder gun used a series of photogates to record the impact velocity. The inferred impact time at the front of the buffer and the measured impact time at the front of the window allowed the transit time of the shock front across the buffer to be determined. Abrupt changes in phase of the Doppler shifted light were also visible in the VISAR and PDV wave profiles when the shock wave reached the rear surface of the buffer. This allowed for an inline determination of the shock velocity. Additionally, in some cases the difference in refractive index between the shocked and unshocked TPX produced a strong enough Fresnel reflection at the shock front that the shock velocity was directly measured using PDV.

In the symmetric impact experiments, the impactor and sample are in the same state immedi-

TABLE I Ambient densities and sound speeds in each of the materials used.

Material	Ambient density (g/cm^3)	Longitudinal sound speed (km/s)	Shear sound speed (km/s)
TPX RT18	0.834 ± 0.001	2.097 ± 0.003	1.023 ± 0.003
TPX DX845	0.831 ± 0.001	2.11 ± 0.01	1.048 ± 0.006
C10100 Cu	8.942 ± 0.005	4.79 ± 0.02	2.30 ± 0.02

TABLE II Thicknesses of impactor, buffer, and window for each experiment.

Experiment	Impactor thickness (mm)	Buffer thickness (mm)	Window thickness (mm)
18-018	2.631 ± 0.001	2.63 ± 0.01	2.633 ± 0.001
18-023	2.855 ± 0.001	2.89 ± 0.01	2.902 ± 0.001
18-620	1.62 ± 0.02	2.783 ± 0.002	2.814 ± 0.001
18-2s16	2.949 ± 0.001	2.802 ± 0.001	2.847 ± 0.001
18-2s19	1.027 ± 0.002	2.838 ± 0.001	2.865 ± 0.001
19-2s19	1.028 ± 0.002	2.885 ± 0.002	2.892 ± 0.002

ately upon impact; the actual particle velocity is simply half of the measured projectile velocity. This is the most accurate method of determining the actual particle velocity, with typical uncertainties of 0.001 km/s. However, it was not possible to achieve high stress states with a symmetric impact due to the low impedance of TPX. For higher stress experiments a copper (alloy C10100) impactor was used. For these experiments, an impedance matching calculation,[13] described in Section III, was used to determine the actual particle velocity. This calculation makes use of the known Hugoniot of the impactor material, and resulted in typical uncertainties of $\sim$0.005 km/s.

III. EXPERIMENTAL RESULTS AND DISCUSSION

A total of six experiments were performed; two on the 101.6 mm bore gas gun, one on the 30.5 mm bore powder gun, and three on the 25.4 mm bore two-stage gun. Three were symmetric impacts (both of the 101.6 mm bore experiments and one of the two-stage experiments), while the remaining three used copper impactors. One of these experiments used TPX grade RT18 and five used grade DX845. For each experiment, the projectile velocity was measured and the apparent

particle velocity was recorded using interferometry techniques. The shock velocity, stress, actual particle velocity, density, and refractive index were inferred from the interferometry data.

A. Mechanical Response

Representative wave profiles for low- and high-stress experiments are shown in Figs. 2 and 3, which used a TPX and copper impactor, respectively. We note that the lower stress experiments exhibited a slight time-dependent response. In particular, the apparent velocity at the impact surface decreased slowly with time, and the apparent velocity at the buffer/window interface displayed slight rounding. This behavior is likely due to a time-dependent viscoelastic response in the material. At higher stresses (5 GPa and above) these features become less apparent. Also visible in the low-stress profiles are abrupt changes in the phase of the Doppler shifted light due to the shock wave reaching the rear surface of the buffer and window. Other differences in the low- and high-stress experiments shown in Figs. 2 and 3 can be attributed to differences in velocity and impactor materials.

The abrupt change in phase of the Doppler shifted light due to the shock wave reaching the rear surface of the buffer and window can be used as a timing fiducial for an inline determination of the shock velocity.[14] The transit of the shock wave through material that has already been partially released due to edge effects may slightly affect the inferred shock velocity; however, the values determined using the inline method are consistent with the shock velocity values inferred using other means, within uncertainty. The time difference between the impact at the edge probes and center probes can also be used to calculate the transit time, though this method has higher uncertainties due to projectile tilt and the need to use interpolation to infer the impact time at the center of the target. In the high-stress experiments the difference in refractive index between the shocked and unshocked TPX produced a strong enough Fresnel reflection at the shock front that sufficient light was reflected from the shock front, enabling direct measurement of the apparent shock velocity, U_S^*. The actual shock velocity, U_S was calculated using $U_S^* = n_0 U_S$, as derived by Dolan,[15] where n_0 is the ambient refractive index at 1550 nm. Uncertainties in the shock velocity calculations were obtained through standard error propagation, and a weighted average of all shock velocity measurements for each experiment is listed in Table III.

FIG. 2 Representative wave profile of a low-stress experiment, in this case 18-023 at ∼1 GPa.

FIG. 3 Representative wave profile of a high-stress experiment, in this case 18-2s19 at ∼19 GPa.

For the symmetric impact experiments, the actual particle velocity is simply half of the measured projectile velocity. For the copper impactor experiments, the actual particle velocity must be determined through impedance matching. At the moment of impact, the TPX sample and the copper impactor are in the same state, so the stress and particle velocity are the same in both. The Rankine-Hugoniot (R-H) jump condition for conservation of momentum can be used to relate the two:

$$P = \rho_0 \, U_S \, u_p. \tag{1}$$

Over the stress range of interest in this study, the shock velocity in copper is well represented by a linear relationship with the particle velocity, u_p. The relationship takes the form U_S = C + Su_p, where the fit parameters for copper are C = 3.970 km/s and S = 1.479 (the low-stress values reported by Knudson and Desjarlais[16]). For TPX, Equation 1 with the measured ambient density ρ_0 and the experimentally determined shock velocity U_S expresses the stress as a function of the actual particle velocity. This results in two equations for the stress in the sample and impactor:

$$P^{TPX} = \rho_0^{TPX} \, U_S^{TPX} \, u_p \tag{2}$$

$$P^{Cu} = \rho_0^{Cu}[C^{Cu}(v_{proj} - u_p) + S^{Cu}(v_{proj} - u_p)^2], \tag{3}$$

where v_{proj} is the projectile velocity. The intersection of these lines determines the stress and actual particle velocity in the shocked state. The values determined through impedance matching are included in Table III for each experiment that used a copper impactor. The uncertainties were determined by a 100000 iteration Monte Carlo simulation which normally varied each parameter within one standard deviation of the measured mean.

Once u_p is known, the R-H jump condition for conservation of mass can be used to determine the density, ρ, in the shocked state:

$$\frac{\rho}{\rho_0} = \frac{U_S}{U_S - u_p}. \tag{4}$$

Figures 4 and 5 show the U_S - u_p and P - ρ results for each of the experiments presented here, compared with previous results for TPX.[10,11] The mechanical response of TPX observed in these experiments agrees well with the results from previous work over the same stress range. As can be seen in Fig. 4, the U_S - u_p response shows no evidence of discontinuity due to transformation or dissociation, in contrast to many other polymers.[17,18] Higher stress data[12] suggests that dissociation occurs in TPX between 40 and 140 GPa. The U_S - u_p response does exhibit slight curvature in

TABLE III Summary of experimental data. First three columns denote the experiment number, impactor material, and sample material, respectively. v_{proj} and U_S are the measured projectile velocity and shock velocity, respectively. u_p, P, ρ, and n are the inferred particle velocity, stress, density, and index of refraction in the peak state, respectively.

Experiment	Impactor	Sample	v_{proj} (km/s)	u_p (km/s)	U_S (km/s)	P (GPa)	ρ (g/cm^3)	n (532 nm)	n (1550 nm)
18-018	TPX RT18	TPX RT18	0.942 ± 0.001	0.471 ± 0.001	2.636 ± 0.003	1.034 ± 0.003	1.014 ± 0.003	1.561 ± 0.001	1.558 ± 0.001
18-023	TPX DX845	TPX DX845	0.939 ± 0.006	0.470 ± 0.003	2.664 ± 0.002	1.039 ± 0.007	1.008 ± 0.002	1.564 ± 0.001	1.559 ± 0.001
18-620	C10100 Cu	TPX DX845	1.490 ± 0.001	1.360 ± 0.001	4.298 ± 0.003	4.85 ± 0.01	1.215 ± 0.001	1.677 ± 0.002	1.674 ± 0.002
18-2s16	TPX DX845	TPX DX845	4.381 ± 0.003	2.191 ± 0.001	5.581 ± 0.007	10.14 ± 0.02	1.366 ± 0.004	1.756 ± 0.001	1.755 ± 0.002
18-2s19	C10100 Cu	TPX DX845	3.670 ± 0.003	3.217 ± 0.004	7.039 ± 0.001	18.81 ± 0.02	1.530 ± 0.002	1.850 ± 0.003	1.846 ± 0.003
19-2s19	C10100 Cu	TPX DX845	5.056 ± 0.004	4.36 ± 0.01	8.582 ± 0.003	31.09 ± 0.07	1.689 ± 0.004	1.95 ± 0.01	1.94 ± 0.01

the low-stress regime, which is common in polymers and may be due to melting.[17,18] Accordingly, the data were fit to a function of the form $U_S = A + B\ u_p - C\ u_p\ e^{-D\ u_p}$; this functional form, the same as that used in Ref. 12, accounts for deviation from linearity at low stress and asymptotes to a linear response at higher stress. These higher precision data at low stress resulted in a slight change in the fit with respect to Ref. 12; the new fit parameters determined using the Monte Carlo method are listed in Table IV along with the correlation matrix.

FIG. 4 U_S - u_p Hugoniot for TPX. Red filled circles denote data from this work, while gray open triangles denote experimental data from Ref. 10 and blue open squares denote DFT calculated data from Ref. 11. The black line is a non-linear fit used in Ref. 12. Fit parameters are found in Table IV

FIG. 5 P - ρ Hugoniot for TPX. Symbols and lines as in Fig. 4.

B. Optical Response

Knowledge of the apparent (u_p^*) and actual (u_p) particle velocities and the shock velocity (U_S) is sufficient to determine the index of refraction in the compressed state provided the material is in a constant state behind the shock front. Under this assumption, the refractive index of a window material compressed by a single shock can be expressed as[19,20]

$$n = \frac{n_0\ U_S - u_p^*}{U_S - u_p}, \tag{5}$$

TABLE IV Fit parameters and correlation matrix for the nonlinear fit shown in Fig. 4: $U_S = A + B\,u_p - C\,u_p\,e^{-D\,u_p}$ determined using the Monte Carlo method.

	A	B	C	D
Fit:	1.659 ± 0.012	1.371 ± 0.003	-0.856 ± 0.021	0.316± 0.005
		Correlation matrix		
A	1.0000	-0.4262	0.9124	-0.6654
B	-0.4262	1.0000	-0.3734	0.7329
C	0.9124	-0.3734	1.0000	-0.8046
D	-0.6654	0.7329	-0.8046	1.0000

where n_0 is the ambient index of refraction. The index of refraction and density in the compressed state were determined for each experiment; these values are listed in Table III and plotted in Fig. 6. The experimentally determined linear relationship over the stress range examined here suggests that the window correction is a constant factor given by the zero-density intercept, a.[21] Using a linear relationship for the refractive index along with Equation 4, Equation 5 simplifies to $u_p^* = a u_p$. The window correction factors were found to be a_{532} = 0.991 ± 0.009 and a_{1550} = 0.997 ± 0.005 at 532 nm and 1550 nm, respectively. This conversion from apparent to actual particle velocity can be used in future experiments up to stresses of 31 GPa.

Because the VISAR and PDV lasers were transmitted through the TPX sample onto the impact surface, a loss of transparency in TPX would have been noticeable through loss of interferometry signal. Since no significant reduction in transmission was observed, we conclude that TPX remained largely transparent at 532 nm and 1550 nm through the entire stress range studied.

FIG. 6 Index of refraction as a function of density for TPX obtained from both VISAR (532 nm, green) and PDV (1550 nm, red). Also shown are linear, least squares fits to the data.

IV. CONCLUSION

Front surface impact and transmission experiments were performed on TPX over the stress range of 1-31 GPa using gas and powder guns. Velocimetry was used to measure the apparent particle velocity and shock velocity, and the actual particle velocity, stress, density, and refractive

index were inferred from the measured shock velocity and impact velocity. The mechanical response in these experiments was found to be in agreement with previously determined Hugoniot results for TPX in this stress range. These measurements also represent a significant improvement in precision. The index of refraction was found to be essentially linear in density. Knowledge of the mechanical and optical properties of TPX enables the calculation of the window correction factors. The constant window correction factors were found to be $a_{532} = 0.991$ and $a_{1550} = 0.997$ at 532 nm and 1550 nm, respectively. TPX was observed to remain optically transparent over the entire stress ranged studied. This study provides the correction factors and material characterization necessary for TPX to be used as a low-impedance optical or x-ray window material for future dynamic compression experiments.

ACKNOWLEDGMENTS

Kurt Zimmerman, Nate Arganbright, Yoshi Toyoda, and Josh Friedman are sincerely thanked for their assistance with these experiments. This publication is based upon work supported by the Department of Energy, National Nuclear Security Administration under Award No. DE-NA0002007.

REFERENCES

[1]J. D. Lytle, G. W. Wilkerson, and J. G. Jaramillo. Appl. Opt. **18**, 1842 (1979).

[2]From Mitsui Chemicals ASTM Physical Properties Table: `https://www.mitsuichemicals.com/tpx.htm`.

[3]From Tydex Optics material data specifications: `http://www.tydexoptics.com/products/thz_optics/thz_materials/`.

[4]L. M. Barker and R. E. Hollenbach. J. Appl. Phys. **43**, 4669 (1972).

[5]O. T. Strand, D. R. Goosman, C. Martinez, T. L. Whitworth, and W. W. Kuhlow. Rev. Sci. Instrum. **77**, 083108 (2006).

[6]M. Naftaly, R. E. Miles, and P. J. Greenslade. "Thz transmission in polymer materials - a data library." 2007 Joint 32nd International Conference on Infrared and Millimeter Waves and the 15th International Conference on Terahertz Electronics (2007).

[7]A. Podzorov and G. Gallot. Appl. Opt. **47**,3254 (2008).

[8]T. D. Aslam, R. Gustavsen, N. Sanchez, and B. D. Bartram. "An equation of state for poly-methylpentene (tpx) including multishock response." AIP Conference Proceedings **1426**, 767 (2012).

[9]T. A. Haill, T. R. Mattsson, S. Root, D. G. Schroen, and D. G. Flicker. "Mesoscale simulation of shocked poly-(4-methyl-1-pentene) (pmp) foams." AIP Conference Proceedings **1426**, 913 (2012).

[10]S. P. Marsh, editor. *LASL Shock Hugoniot Data*. University of California Press, Berkeley, (1980).

[11]T. R. Mattsson, J. M. D. Lane, K. R. Cochrane, M. P. Desjarlais, A. P. Thompson, F. Pierce, and G. S. Grest. Phys. Rev. B **81**, 054103 (2010).

[12]S. Root, T. R. Mattsson, K. Cochrane, R. W. Lemke, and M. D. Knudson. J. Appl. Phys. **118**, 205901 (2015).

[13]A. C. Mitchell and W. J. Nellis. J. Appl. Phys. **52**, 3363 (1981).

[14]S. C. Jones and Y. M. Gupta. J. Appl. Phys. **88**, 5671 (2000).

[15]D. H. Dolan. Foundations of VISAR analysis. Technical report, Sandia National Laboratories, (2006).

[16]M. D. Knudson and M. P. Desjarlais. Phys. Rev. B **88**, 184107 (2013).

[17]N. K. Bourne. Journal of Dynamic Behavior of Materials **2**, 33, (2016).

[18]D. M. Dattelbaum and J. D. Coe. Polymers **11**, 493 (2019).

[19]D. R. Hardesty. J. Appl. Phys. **47**, 1994 (1976).

[20]R. E. Setchell. J. Appl. Phys. **50**, 8186 (1979).

[21]D. Hayes. J. Appl. Phys. **89**, 6484 (2001).

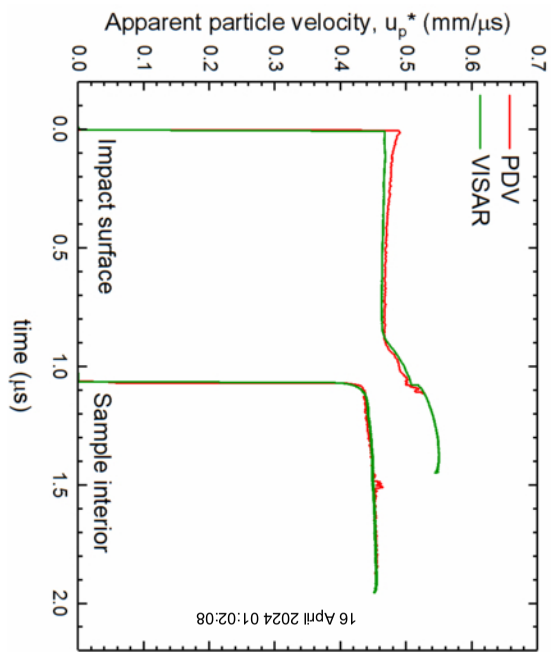

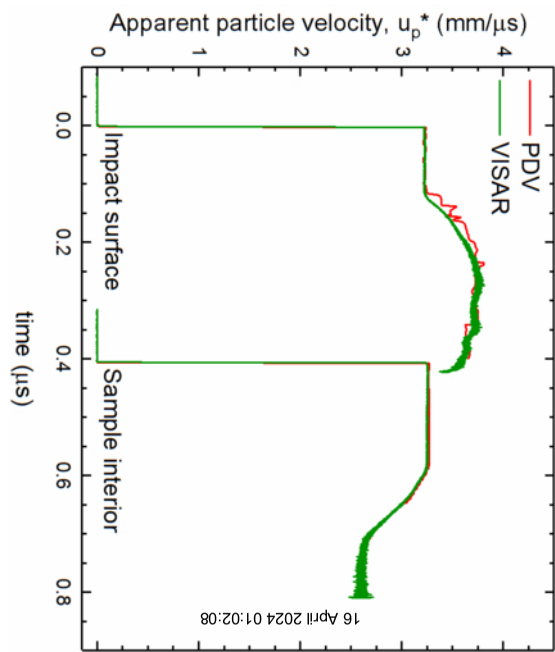

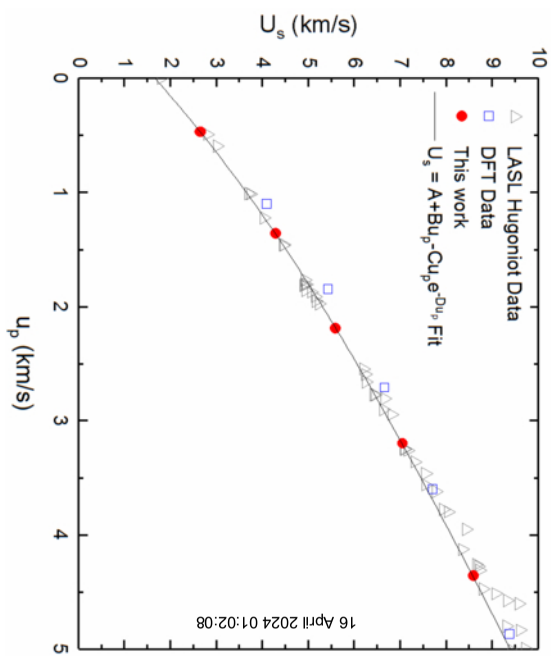

PLEASE CITE THIS ARTICLE AS DOI: 10.1063/1.5127867